Journal of Engg. Research **Vol. 5 No. (6) March 2018 pp.** *1-14*

تقدير الضغط التشبعي لمكامن النفط بطريقة فعالة باستخدام وبناء نماذج تركيبية بسيطة

د. حسن احمد الكندري، أ.د. عادل محمد الشرقاوي، د. عادل حسين مال الله، د. اسامه علي العمير

قسم هندسة البترول – كلية الهندسة والبترول – جامعة الكويت

صندوق بريد 5969 الصفاة – دول الكويت

الخلاصة

قياسات ضغط التشبع حاسمة لجميع سوائل المكامن الهيدروكربونية. يصل ضغط الغاز إلى التشبع الحرج وذلك عند انخفاض ضغط النفط إلى اقل من ضغط التشبع . بعدها يصل المكمن الى حالة التدفق الثنائي والذي ينتج عنه انخفاض كمية إنتاج النفط الكلي. ولزيادة إنتاج كميات اضافية من النفط، يجب المحافظة على تقارب ضغط المكمن الى ضغط التشبع الاولي. وأفضل طريقة لقياس ضغط المكمن هو باستخدام عينات من قاع المكمن أو إعادة مزج عينات النفط والغاز بالسطح. وفي بعض الأحيان، لا يمكن الحصول على هذه العينات وتكون تقديرات الضغط بطرق حسابية.

في هذه الدراسة تم استخدام عدد كبير من العينات وصل الى 231 تركيب نفط خام وقياس ضغط التشبع من خلال استخدام البيانات المنشورة في المجلات العلمية وكذلك بيانات غير منشورة بالسابق بالإضافة الى البيانات المقاسة خصيصا لعمل هذا البحث ومن ثم تم استخدامها بنموذجين تم اعدادهما للتنبؤ بضغط التشبع من مجموعة متنوعة من الزيوت الخام. وتم استخدام جميع المركبات الهيدروكربونية من الميثان الى الهيبتان+ بالإضافة الى الشوائب الغير هيدروكربونية بالنموذج الاول. وتم استحداث النموذج الثاني عن طريق جمع التراكيب الخفيفة مع بعضها وكذلك المتوسطة والثقيلة بالإضافة إلى العناصر الغير هيدروكربونية. وتم بعد ذلك مقارنة أداء النماذج إلى كل من «بنغ روبنسون» و «سوافى-ريدش-وانغ» بالإضافة إلى جميع الطرق المنشورة في هذا المجال الى تاريخ نشر هذا البحث من خلال مقارنة هذه النماذج مع ما هو منشور ومعروف بالسابق. تم التوصل والاثبات بان النموذجين المقترحين هما أبسط وأكثر دقة من الطرق الحسابية المنشورة سابقا.

Simple and efficient compositional based models to estimate the saturation pressure of oil reservoirs

Hassan Alkandari*, Adel Elsharkawy, Adel Malallah and Osamah Alomair

Petroleum Engineering Department, College of Engineering & Petroleum,

Kuwait University, P.O. Box 5969, Safat 13060, Kuwait

** Corresponding Author: Hassan@hkandari.com*

Abstract

Saturation-pressure measurements are essential for all hydrocarbon reservoir fluids. Gas reaches a critical saturation, below the crude oil saturation pressure; then, a two-phase flow takes place and this action results in decreasing oil production and recovery. One of the reservoir engineers goals is to optimize the production of oil and to maximize oil recovery; to reach this goal, the reservoir pressure must be retained very close to the initial reservoir saturation pressure. Saturation pressure is normally measured by using a bottom-hole samples or samples that are recombination of gas and oil at surface. In most cases, real samples are unavailable at elevated pressures; therefore, saturation pressure needs to be estimated either by simulation or computation methods.

A set of crude oil saturation pressure and composition measurements including data from the literature and newly measured data were used to develop two practical models to predict the saturation pressure of a 214 crude oils. The first developed model uses the extended compositions of hydrocarbons up to the heptane plus fraction in addition to non-hydrocarbons. The second model utilizes the lumping criteria for compositions of light components, intermediate components, and heavy components in addition to non-hydrocarbon components as an input. The models' performance is also compared to the Soave-Redlich-Kwong and Peng-Robinson equation-of-states in addition to published methods that use compositions as an input. The comparison indicates that the proposed models are easier to implement and more accurate than the other computational methods.

Keywords: Saturation pressure (Ps); bubble-point pressure (BPP); equation of state (EOS); correlations; PVT data.

Introduction

Reservoir fluid properties are an essential source of information for all calculations on hydrocarbon reserves. Accurate estimation of the pressure-volume-temperature (PVT) measurement is crucial. Of all the PVT properties, saturation pressure (Ps) is considered the most important parameter. It is well known that gas starts to flow once the reservoir pressure drops below the bubble point pressure, and the gas saturation reaches a critical value. To minimize the gas flow and maximize the oil recovery, it is very important to maintain the reservoir pressure close to the original bubble point pressure. Although the PVT properties are experimentally measured in laboratories and provide reliable results, this process is expensive, time consuming, and sometimes unavailable; therefore, measured field data (separator gas oil ratio, separator pressure, stock-tank oil specific gravity, and reservoir temperature) or reservoir fluid compositions are used to estimate the bubble point pressure.

There are two methods in the petroleum industry to estimate the saturation pressure of crude oil when experimental data is unavailable, either using production data or compositional data.

Methods based on production data (composition is unavailable)

Numerous attempts have been made since the 1940s to develop correlations to estimate the saturation pressure from production data, such as producing gas oil ratio, oil gravity, gas gravity, reservoir pressure, and temperature.

Methods based on compositional data

Many authors have reported that the application of any correlation in other regions results in serious errors. These conclusions arise from the fact that regional crude oils represent a physical-chemical trend; therefore, all attempts to develop a general correlation using field measured parameters to estimate the saturation pressure from a large data bank have failed. For this reason, Elsharkawy (2003) made the first attempt to correlate the saturation pressure to the reservoir fluid composition instead of using the production data. In recent years, there have been several attempts to estimate the saturation pressure of oil reservoirs, which will be one of the tasks of this paper.

Elsharkawy presented a correlation of the bubble point pressure for the oil reservoir using the same input data needed for the equation-of-state (EOS) calculations, that is, the compositional data and the reservoir temperature. Elsharkawy's model is based on the saturation pressure measurements of 60 crude oil samples from the Middle East and 75 collected from the literature.

AlQuraishi (2009) attempted to model the saturation pressure using Elsharkawy's data. The model was developed using linear genetic programming. He correlated the saturation pressure to the formation temperature, methane content, and heptanes plus molecular weight. Thus, AlQuraishi's model neglected the effect of the intermediate and heptane plus content on the saturation pressure. The error analysis reported by AlQuraishi indicates that his model has a 5.8% error compared to 7.7% by Elsharkawy, 9.9% using the SRK-EOS, and10.1% using the PR-EOS.

Bandyopadhyay and Sharma (2011) presented a model to predict the bubble point pressure, using temperature and fluid composition. They used 129 experimental and literature data originally published by Elsharkawy (2003) to develop their model. The model introduced a temperature interaction parameter that depends on compositions. The proposed model has a set of 24 coefficients and the estimated bubble point pressure is calculated as the sum of the series calculations. They reported an average absolute error (AAR) of 7.83% using their model compared to 8.3% using Elsharkawy's simple model (2003), 10.15% using SRK-EOS, and 10.58%using the PR-EOS.

Farasat et al. (2013) presented a new mathematical approach to calculate the crude oil saturation pressure as a function of the temperature and the reservoir fluid composition. The model developed by Farasat et al. used 130 experimental data, which were originally published by Elsharkawy (2003). Farasat used a support vector machine (SVM) to model the saturation pressure. They did not clearly demonstrate how to calculate the saturation pressure from the SVM model. Moreover, they did not indicate the overall average absolute deviation (AAD) for their model compared to other published models and both the PR-EOS and SRK-EOS.

Ahmadi et al. (2014) also presented an ANN technique called gene expression programming (GEP) to determine the bubble point pressure of the oil samples. Similar to Farasat et al. (2013), Ahmadi's model used most of the data previously published by Elsharkawy (2003) to construct a non-linear equation using reservoir fluid compositions and temperatures as input parameters. The proposed model is highly complicated and consists of 8 equations that have several constants compared to the one simple equation proposed by Elsharkawy (2003). They compared the performance of their proposed model to the SRK-EOS and PR-EOS; however, their paper does not mention how the heptanes plus fraction was treated and characterized for the EOS calculations. They reported an AAD of 4% using the proposed model compared to 8% using Elsharkawy's model (2003), 10.9% by PR-EOS, 10.5% by SRK-EOS, and 15% by Bandyopadhyay and Sharma (2011).

Gholami et al. (2014) estimated the bubble point pressure using a "support vector regression SVR and a supervised learning algorithm SLT based on the statistical learning theory", and then the ACE was used. The model used reservoir fluid compositions and temperature to estimate the bubble point pressure. Gholami et al. (2014) used the same data originally published by Elsharkawy (2003). They presented three attempts based on genetic programming to correlate the bubble point pressure: SVR, ACE, and power-law committee machine (PLCM). The ACE-based method resulted in a set of three equations with a matrix of [8 by14] constants. Gholami et al. (2014) compared the accuracy of their model to the SRK-EOS and PR-EOS predictions reported by Elsharkawy (2003). Based on their AARD analysis, the PLCM model has the lowest errors followed by the SVR model, Elsharkawy's model, ACE model, PR-EOS, and SRK-EOS.

Lately, Jarrahian et al. (2015) presented two empirical models to estimate the saturation pressure of black oils. The first model is based on production information. The second model is based on compositional information mostly from Elsharkawy1 (2003) and Heidaryan and Moghadasi (2011). They have not presented a comparison of the accuracy of their model to Farasat (2013) model, Ahmadi (2014) model, and Gholami (2014) model.

This paper is concerned with the estimation of saturation pressure using compositional data. Therefore, the objective is to develop a simple, yet robust model to estimate the saturation pressure for various types of reservoir oils using a larger data bank than that used by other published studies. The accuracy of the proposed models is compared to previously published models as well as SRK-EOS and PR-EOS.

Data bank

This paper uses 231 data sets of crude oil saturation pressure and compositions measurements. The data set consists of 130 data sets originally reported by Elsharkawy (2003) in addition to others collected from the literature, 94 new data sets that have not been published; as well as 7 newly measured samples at the Petroleum Fluid Research Center (PFRC) in Kuwait University. These data represent a wide range of compositions, such as volatile oils, black oils, and heavy oils. The data range of pressure is from 537 to 5065 psia and temperatures ranging from 58 to 319oF, crude oil compositions from C1 to C7+, non-hydrocarbons, such as N2, H2S, and CO2, and the molecular weight and the specific gravity of the heptane plus fraction.

Data classification and screening

The compositions and the saturation pressure measurements in the data bank are subjected to a meticulous screening process to check the validity of the data. Our screening criteria uses the following steps: the sum of the molar compositions of all the components must add up to one; otherwise, the sample is eliminated.

After filtering, data were reduced to 214 and divided into 179 measurements used to develop the new models, and 35 data sets are used for the blind test of the robustness of the proposed models. Statistical analysis of the input variables of the data set used in training and testing the extended and the lumped models are illustrated in Table 1.

Table 1. Description of the data used to develop and test the extended model.

Input	179) Training model (Data			(Data 28) Testing			new 7) Testing (experimental		
	.Min	.Ave	.Max	.Min	.Ave	.Max	.Min	.Ave	.Max
N2	0	0.35	1.67	0	0.27	1.67	0.10	0.26	0.35
CO2	0	1.27	11.37	0	1.17	11.37	0.14	0.41	0.83
H2S	0	0.15	3.68	0	0.15	3.22	0.00	0.00	0.00
C1	13.16	33.86	74.18	19.50	34.79	73.36	20.64	28.25	42.79
C2	3.36	8.07	13.71	4.64	8.26	11.63	6.69	7.88	10.82
C3	0.89	6.59	11.87	2.46	6.76	12.03	6.05	6.59	7.10
C4	0.95	4.46	8.4	1.66	4.41	6.58	4.03	5.05	5.93
C5	0.40	3.21	5.95	1.00	3.11	5.23	3.36	4.33	5.52
C6	0.00	3.14	6.37	0.99	3.15	5.46	2.88	3.74	4.33
+C7	10.72	38.89	57.73	11.18	37.88	51.22	27.61	43.49	51.31
+SG.C7	0.74	0.87	0.959	0.70	0.86	0.93	0.85	0.89	0.92
+MWC7	134	240	368.9	105	223	292	216	262	298
T, o F	58	156	319	58	165	261	121	157	230
Ps, psia	537	2198	5065	1025	2307	5000	1227	1779	3344

Several of the reported compositional data have extended analysis up to (C_{20+}). The following techniques are used for lumping or regrouping the extended analysis into single pseudo-fractions (C_{7+}). "The mole fraction (X_i) of the individual components of the extended analysis is equal to the plus fraction" (Ahmad, 2011).

$$X_{C_{7+}} = \sum_{i=7}^{n} X_i \qquad \text{i=7, 8 … n} \tag{1}$$

The molecular weight average (Mw) of the single component of model is equal to the molecular weight of the heptanes plus fraction.

$$Mw_{C_{7+}} = \sum_{i=7}^{n} \frac{X_i Mw_i}{X_{C_{7+}}} \qquad \text{i=7, 8 … n} \tag{2}$$

The density of the total heptane plus-fraction (g_{C7+}) can be calculated as follows:

$$\gamma_{C_{7+}} = \frac{X_{C_{7+}} Mw_{C_{7+}}}{\sum_{i=7}^{n} \frac{X_i Mw_i}{\gamma_i}} \qquad \text{i=7, 8 … n} \tag{3}$$

It is important to note the significance of the density of plus fraction because its density determines its paraffinic naphthenic aromatic (PNA) content.

Equation-of-state calculations

The EOS calculation of the saturation pressure is compared with the newly developed models as well as the other methods. The two EOS calculations considered in this paper are the ones most considered and widely used in the petroleum industry to evaluate the volumetric and phase behavior of reservoir fluid properties: the (Soave-Redlich-Kwong, 1972) EOS (SRK-EOS) and the (Peng-Robinson, 1976) EOS (PR-EOS). It should be noted that the accuracy of any EOS calculation of the saturation pressure largely depends on the number of pseudo-components and the splitting schemes used to divide the heptane plus fraction. Therefore, both calculations using EOS to estimate the saturation pressure will not lead to similar results, even though the number of pseudo-components, characterization of the pseudo-components, and binary interaction parameters were the same. Appendix A is given to show details of the EOS calculation, splitting the hydrocarbon fraction, characterization of the sub-fractions and the binary interaction numbers.

Model development

As previously stated, the objective of this work is to provide the petroleum reservoir engineer with a simple, yet accurate tool to estimate the saturation pressure for a variety of crude oils using compositional data when experimental is unavailable. Two models are presented in this study to calculate the saturation pressure of the crude oil samples. The first model uses all input parameters, such as the molar compositions of the hydrocarbon and non-hydrocarbon components similar to the EOS models. This model is referred to as the extended model. The second model uses fewer input parameters in which some of the hydrocarbon components have been lumped into a single group; this is designated as the lumped model. Both models are simpler than all published correlations, physically correct, and have an acceptable accuracy compared with the well-known EOS.

Figure 1 shows a correlation matrix of all the data available under consideration. This figure also indicates the relative importance of each of the input variables into the first proposed model. It agrees with most published correlations and the EOS that the methane content, heptane plus content, and temperatures have the greatest impact on the saturation pressure, followed by the intermediate content. The data understudy indicates that the non-hydrocarbon has the smallest impact. This result is simply a reflection of the molar contribution of each component comprising the crude oil composition.

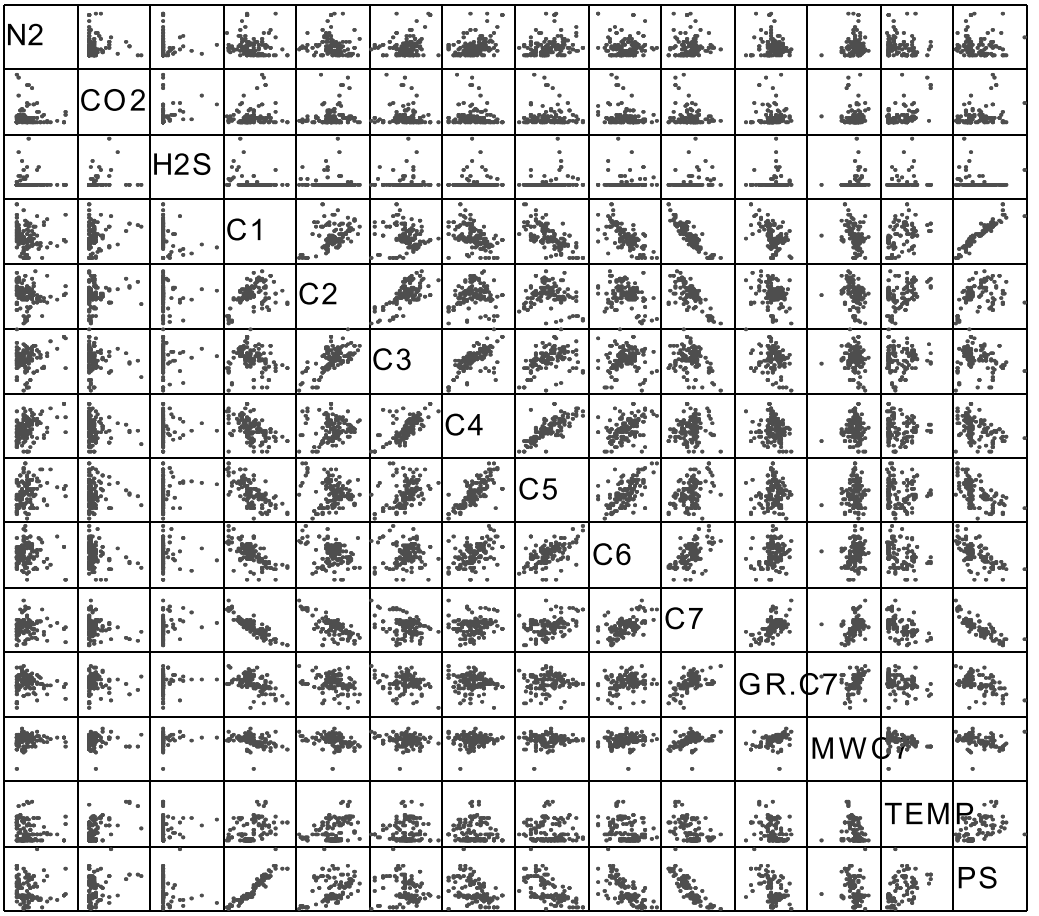

Figure 1. Correlation matrix for all the variables in the oil data bank.

Model I- extended model

The extended model uses 13 variables comprising the molar compositions of the pure components, heptane plus properties, and reservoir temperatures, which are similar to the input parameters for the EOS. Figure 2 shows the correlation coefficient graph of all the input parameters in the extended model. Thus, the elimination of the intermediate effect has a negative impact on the accuracy of the predictive model. Our proposed extended model has the following form:

$$Ps = 124.72N_2 + 17.57CO_2 + 22.55H_2S + 64.22C_1 - 9.80C_2 - 52.49C_3 + 6.16C_4 - 19.22C_5 - 23.63C_6$$

$$- 21.43C_{7+} + 435.31g_{C7+} + 1.14Mw_{C7+} + 4.29T \quad (4)$$

where T is the temperature in °F, Ps is the saturation pressure in psia, and the hydrocarbon and non-hydrocarbon compositions are expressed in mole percent.

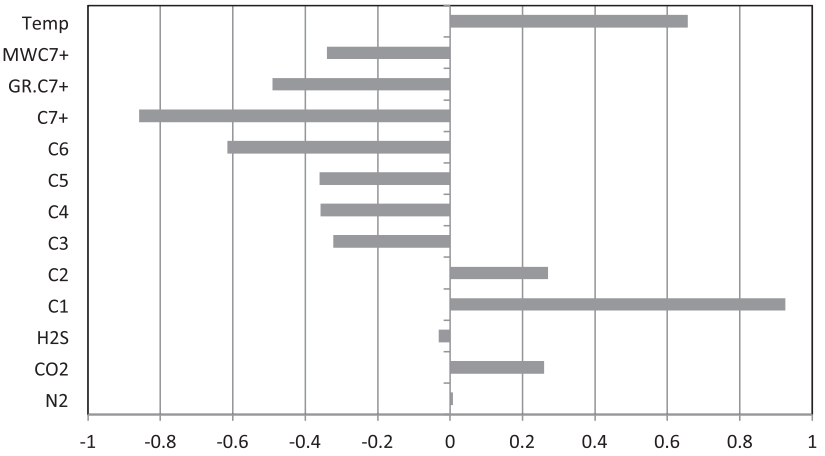

Figure 2. Correlation coefficient for all the variables in the training model (179 data).

Model II-lumped model

The second model (lumped model) is much simpler and uses only 7 variables. Several lumping schemes are adapted in the petroleum industry for phase behavior modeling and reservoir simulation of the petroleum reservoir fluids (Ahmed, 2011). Hydrocarbon components are grouped into a pseudo fraction based on their molecular weight (Whitson, 1980), the similarity of their physical-chemical properties (Lee, 1979), their carbon number, their true boiling point, or their number of families based on the chemical structure (Becker et al., 2015). Emera and Samara (2005) proposed lumping the hydrocarbon components into volatile (C_1+N_2), intermediate (CO_2, H_2S, C_2 to C_4) and heavy categories (C_{5+}) to calculate the minimum miscibility pressure. Duan et al. (2013) proposed lumping several components into a single carbon number (SCN) with predetermined values for properties, such as critical pressure, temperature, and eccentric factor. Others have proposed optimal lumping schemes based on the objectives (Lin et al., 2008). In lumped model, C_1+N_2, C_2, CO_2, and H_2S, the intermediate ($C_3$to C_6), heptanes plus (C_{7+}) and its properties, and temperature are the input variables. The correlation matrixes of the lumped components are provided in Figure 3. Even though the non-hydrocarbon has the least effect, their contribution is important, especially the H2S in the case of sour crudes.

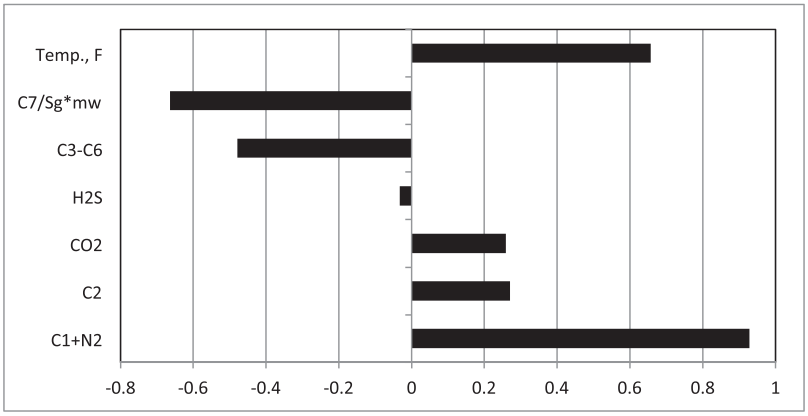

Figure 3. Correlation matrix for the lumped model (179 data).

Both models presented by AlQuraishi (2009) and Bandyopadhyay and Sharma (2011) have eliminated the effect of H2S. The proposed model has the following form:

$$Ps= 82.115(C_1+N2)-11.635C_2+39.158CO_2+ 38.244H_2S -1.217(C_3\ldots C_6) -890.701(C_{7+}/MW_{7+}*\gamma_{7+}) + 4.217T-1042 \quad (5)$$

where T is the temperature in °F, Ps is the saturation pressure in psia, and the hydrocarbon and non-hydrocarbon compositions are expressed in mole percent.

Result and discussion

Model accuracy

The accuracy of the two proposed models used to estimate the saturation pressures of the previously described crude oil samples is shown in Table 2 using new compositional and saturation pressure data. This table shows the average relative error, average absolute relative error, standard deviation, and the correlation coefficients for all the methods considered in this study. Details of the equations used are given in Appendix B. Table 2 also reports the accuracy of the PR-EOS, SRK-EOS, Elsharkawy's (2003) model, AlQuraishi's (2009) model, Bandyopadhyayand Sharma's (2011) model, and Jarrahian's (2015) model. The methods proposed by Gholami et al. (2014), Ahmadi et al. (2014), and Jarrahian et al. (2015) are included in Table 2, even though they produce an unreasonable estimate of the saturation pressures, as explained in appendix C.

Table 2. Error analysis of the proposed models in comparison with all the investigated methods.

Method	%ARE	%AARE	SEE	%R2
PR-EOS	6.24	10.19	14.13	92.65
SRK-EOS	3.12-	10.36	15.91	92.80
(2003) Elsharkawy	0.85	8.57	14.10	93.58
(2009) AlQuraishi	9.36-	11.37	17.52	90.61
(2011) Bandyopadhyay	8.05	12.28	17.83	90.82
(2014) .Gholami et al	?	?	?	?
(2014) .Ahmadi et al	?	?	?	?
(2015) Jarrahian et al	35.52	35.56	38.68	27.38
New Extended Model	0.11	7.84	12.08	95.37
New Lumped Model	0.19	7.81	12.24	94.90

This table indicates that the extended and the lumped models have an AARE in the order of 7.84% and 7.81%, respectively. It should be noted that the complications in the Bandyopadhyay and Sharma (2011) model did not improve the accuracy of the saturation pressure, because it had a large error. It is also noted that Jarrahian et al. (2015) model produces an average error of 36%. Compared with the EOS, the lumped model has a few constants and eliminates the splitting, characterizing the pseudo-components and binary interaction parameters necessary for the EOS calculations. The lumped model as well as the extended model is very simple and requires one-step calculations compared with all the other methods reported in Table 3.

A cross-plot of the calculated saturation pressure using the extended model based on the training data versus the measured data is illustrated in Figure 4A. This figure indicates that most of the data falls on the unit slope line, and there is no over-fit.

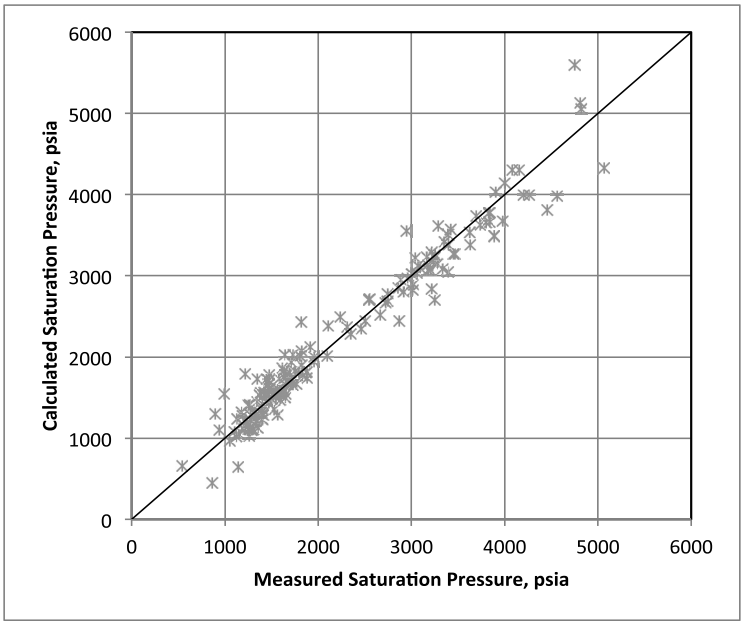

Figure 4A. Cross plot of the extended model using 179 training data.

This trend is supported by the high correlation of regression of the model (95.4%) presented in Table 2. Figure 4B shows a cross-plot of the testing data (28 from the literature and 7 new measured in PFRC at Kuwait University).

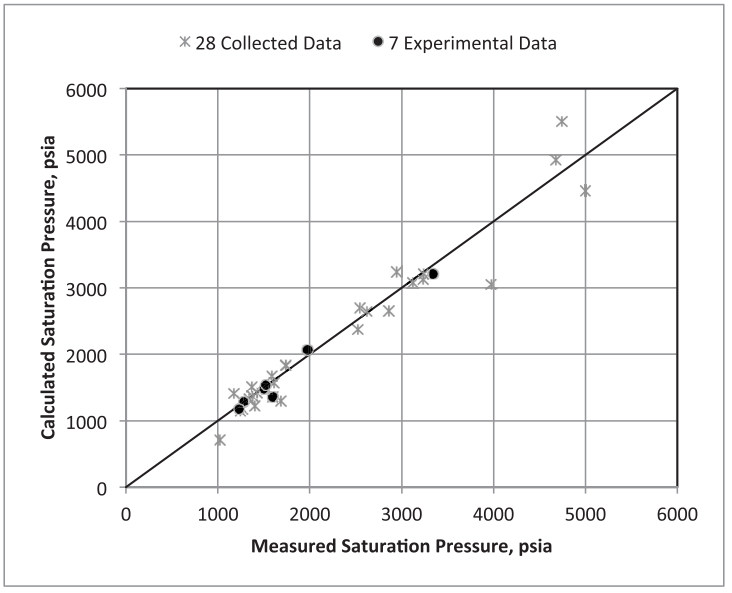

Figure 4B. Cross-plot of the extended model using 35-testing data.

The extended model indicates an excellent agreement with all of the 28 data sets chosen at random, with the exception of a few data points at higher pressures. Additionally, the model has a good match for the 7 newly measured samples.

Figure 5A shows the performance of the lumped training-model for capturing the measured saturation pressure for most of the 179 samples.

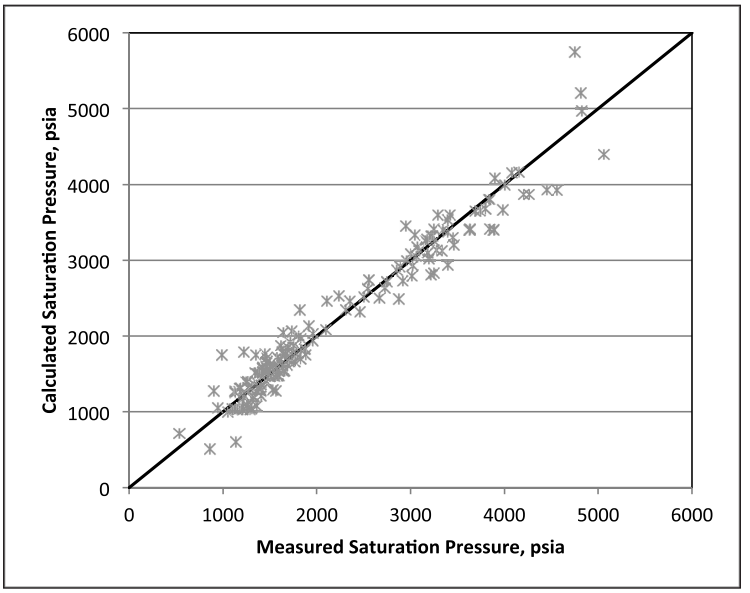

Figure 5A. Cross-plot of the lumped model using 179 training data.

A cross-plot of the calculated saturation pressure using the lumped model based on the training data versus measured data is depicted in Figure 5B.

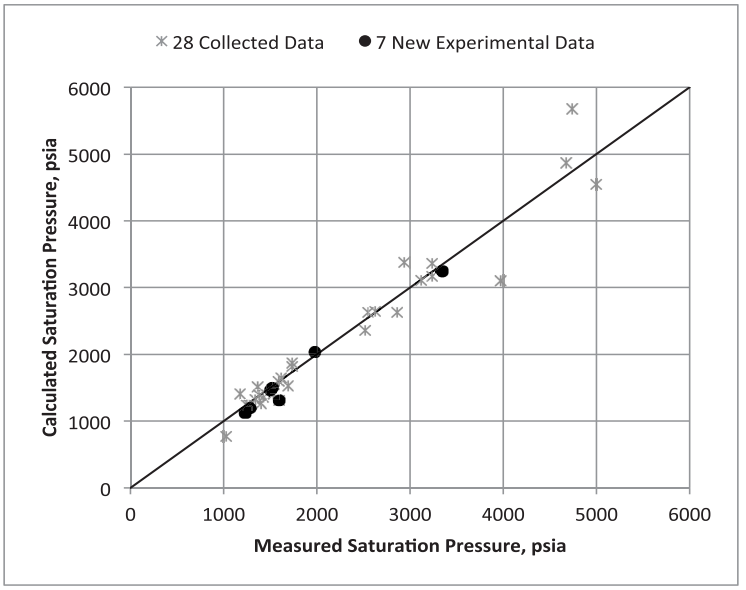

Figure 5B. Cross-plot of testing data for the lumped model.

This figure indicates that most of the data scatters fall into the unit slope line. The lumped model also has a high coefficient of regression of 95%, which is indicated in Table 2.

Models validity

The accuracy and validity of the two newly introduced models to estimate saturation pressures of various types of oil are reported in Table 3. This table illustrates the capability of the newly proposed models to predict the saturation pressure for volatile oils, and black oils. Table 3 provides the compositions, properties of the heptane plus fraction, temperature, and measured saturation pressures of the samples. Additionally, the calculated saturation pressure using the PR-EOS (1976) model, SRK-EOS (1972) model, Elsharkawy's (2003) model, AlQuraishi's (2009) model, Bandyopadhyay and Sharmas (2011) model, and Jarrahian et al. (2009); and the extended and lumped models are provided in Table 3. It is clear from this table that the proposed models have a wide range of applications regardless of the crude oil types. We have also included information regarding the 7 newly measured data sets, at the PFRC, compositional, and saturation pressure. At the bottom of Table 4, we have provided the unpublished data of the compositions and the saturation pressures at low temperatures. It is well known that the saturation pressure of a crude sample is measured at low temperatures in addition to the reservoir temperature as a method to check the quality of the sample.

Table 3. Comparing model accuracy for calculations of saturation pressures for various crude oils.

Volatile-Oil-Samples (C7+<30)																						
Fluid Source	index	N2	CO2	H2S	C1	C2	C3	C4	C5	C6	C7+	GR.C7+	MWC7+	T, °F	Ps, psi	SRK	PR	Elsh	Alq	Bandy	Jarr	Extd	Lump
Rosenegger	7	0.03	8.39	0	47.4	10.3	6.12	4.2	2.89	2.05	18.6	0.83	180	295	4000	3933	3879	4460	4420	4165	3317	4128	4178
Vogel-80	13	0.65	0.02	0	45	12.5	8.93	6.03	3.02	1.44	22.4	0.81	184	140	3002	2624	2548	2742	2895	2643	1812	3008	2996
Dansh-92	18	0	0	0	46.8	8.77	7.44	4.01	2.56	4.02	26.4	0.77	158	212	2941	2550	2594	3248	3617	3269	1944	3269	3374
Middle East	31	0.44	0.38	0	49.1	7.6	6.13	3.84	2.52	2	28	0.84	231	199	3739	3522	3507	3418	3951	3508	2309	3629	3644
Middle East	45	0.03	0.97	0	41.6	10.8	7.52	4.5	3	2.43	29.1	0.85	208	241	3069	3109	2979	3080	3513	3138	1962	3122	3140
Coats-86	51	0.55	1.03	0	36.5	9.93	8.85	6	3.78	3.56	30.4	0.84	200	234	2746	2537	2472	2714	2945	2643	1682	2696	2720

Black-Oil -Samples (35<C7+<55)																						
Fluid Source	index	N2	CO2	H2S	C1	C2	C3	C4	C5	C6	C7+	GR.C7+	MWC7+	T, °F	Ps, psi	SRK	PR	Elsh	Alq	Bandy	Jarr	Extd	Lump
Coats-86	73	1.64	0.08	0	28.4	7.16	10.5	8.4	3.82	4.05	36	0.84	252	131	1694	1674	1618	1615	1738	1644	1084	1735	1713
Middle East	88	0.08	1.37	0.69	36	8.67	5.94	2.97	1.5	3.1	39.7	0.9	274	168	2505	2710	2318	2247	2608	2321	1476	2455	2445
Middle East	114	0.29	0.48	0	28.4	8.29	7.38	5.06	3.42	4.41	42.3	0.88	252	133	1632	1672	1477	1544	1748	1517	984	1595	1598
Middle East	122	0	1.25	0	33.4	9.24	6.07	2.4	1.62	2.78	43.3	0.85	252	230	2110	2313	2278	2424	2737	2438	1410	2392	2412
Middle East	134	0	0.17	0	28.6	8.63	7.43	3.81	2.61	4.11	44.7	0.86	249	134	1548	1551	1429	1477	1764	1433	937	1516	1567
Middle East	146	0.44	0.83	0	27.8	7.54	6.9	4.61	3.1	3.11	45.7	0.9	272	133	1565	1799	1505	1558	1730	1528	1002	1607	1590
moharam-96	149	0.21	0.34	0	20	7.93	8	6.6	5.87	5.08	45.9	0.86	230	235	900	1353	1290	1531	1514	1225	773	1288	1294
Middle East	162	0.35	0.47	0	26.5	7.71	6.05	4.03	4.08	4.22	46.6	0.89	253	135	1500	1613	1380	1427	1631	1391	923	1464	1456
Middle East	176	0.12	0.51	0	28.8	7.91	6.46	3.17	2.07	3.25	47.7	0.88	250	134	1615	1665	1476	1574	1783	1502	981	1581	1614
Middle East	194	0.21	0.15	0	27.8	7.68	6.19	3.41	1.81	2.84	49.9	0.86	228	134	1590	1532	1377	1545	1680	1426	923	1473	1493
Rosenegger	207	0.37	0.02	0	17.3	6.11	8.23	5.47	3.76	3.96	54.8	0.85	242	156	537	938	888	914	1064	836	558	674	731

Newly-Measured Kuwait University Laboratory																						
Fluid Source	index	N2	CO2	H2S	C1	C2	C3	C4	C5	C6	C7+	GR.C7+	MWC7+	T, °F	Ps, psi	SRK	PR	Elsh	Alq	Bandy	Jarr	Extd	Lump
KU-1	209	0.33	0.22	0	25.6	6.87	6.39	5.61	4.68	4.33	46	0.879	222	133	1595	1360	1530	1442	1514	1394	860	1349	1337
KU-2	210	0.35	0.47	0	26.5	7.71	6.05	4.03	4.08	4.22	46.6	0.893	253	135	1500	1400	1620	1427	1631	1391	924	1465	1456
KU-3	211	0.27	0.74	0	23.1	7.2	6.45	5.93	4.66	4.16	47.5	0.906	290	138	1283	1140	1360	1284	1448	1296	800	1269	1219
KU-4	212	0.22	0.26	0	20.6	6.69	6.65	5.11	5.52	3.6	51.3	0.919	298	171	1227	1120	1300	1188	1415	1170	742	1155	1131
KU-5	213	0.19	0.14	0	27.8	8.37	6.88	5.28	4.33	3.85	43.2	0.89	278	121	1524	1300	1560	1402	1659	1409	928	1524	1489
KU-6	214	0.33	0.24	0	31.3	7.48	6.58	4.86	3.7	3.17	42.3	0.9	274	171	1978	1800	2200	1975	2242	1985	1224	2052	2026
KU-7	215	0.1	0.83	0	42.8	10.8	7.1	4.51	3.36	2.88	27.6	0.85	216	230	3344	3070	3400	3083	3568	3139	2003	3204	3200

Low-Temperature Oil Samples (59°F<T<71°F)																						
Fluid Source	index	N2	CO2	H2S	C1	C2	C3	C4	C5	C6	C7+	GR.C7+	MWC7+	T, °F	Ps, psi	SRK	PR	Elsh	Alq	Bandy	Jarr	Extd	Lump
Middle East	101	0	1.12	0.21	27	10.8	9.23	4.97	2.62	3.33	40.8	0.88	249	71	1247	1090	1033	1040	1235	564	808	1167	1205
Middle East	117	0.36	0.17	0	27.2	8.93	8.6	6.07	3.71	2.55	42.4	0.88	271	68	1130	1028	1245	1094	1248	766	820	1230	1228
Middle East	135	0	0.17	0	28.6	8.63	7.43	3.81	2.61	4.11	44.7	0.86	249	70	1270	1055	1255	1130	1311	783	826	1242	1297
Middle East	138	0.14	0.54	0	29.4	7.96	6.19	3.96	3.25	3.84	44.7	0.9	290	59	1265	1065	1350	1191	1301	880	894	1401	1390
Middle East	147	0.44	0.83	0	27.8	7.54	6.9	4.61	3.1	3.11	45.7	0.9	272	67	1320	1125	1400	1201	1268	921	879	1324	1312
Middle East	173	0.06	0.81	0	31.3	7.42	5.68	2.82	1.63	2.64	47.6	0.89	270	68	1460	1215	1535	1441	1463	1026	975	1550	1576
Middle East	193	0.16	0.3	0	24.7	7.51	6.92	4.76	2.65	3.43	49.6	0.88	239	71	1050	975	1156	1008	1107	701	714	969	986

Elsh: Elsharkawy[1] (2003) Alq: AlQuraishi[3] (2009) Band: Bandyopadhyay and Sharma[4] (2011) Jarr: Jarrahian et. al.[9] (2015)
Extd: Extended model Lump: Lumped model

Figure 6A reports the error of all the methods considered in this paper to predict the saturation pressure for volatile oils (heptane plus content below 30%).

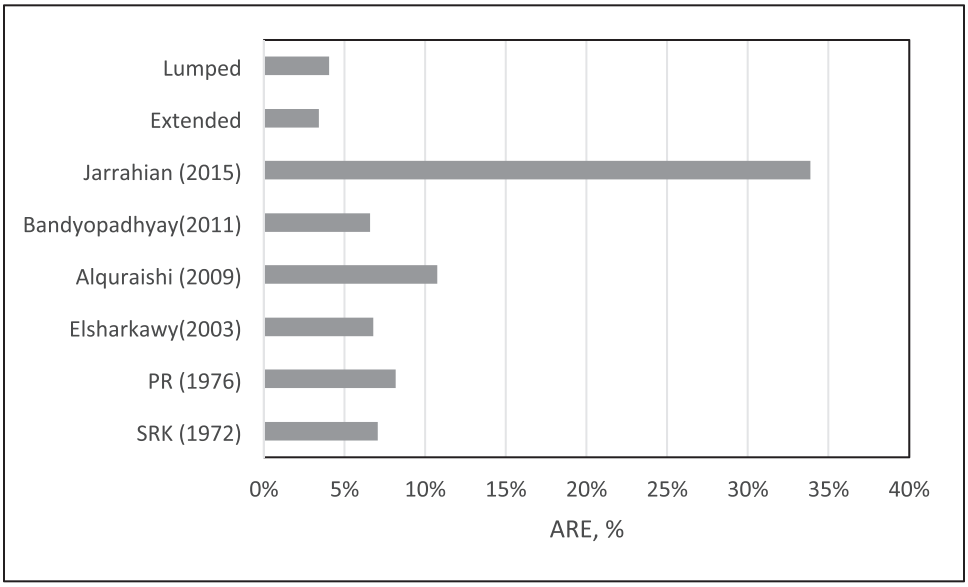

Figure 6A. Comparison of all the models' accuracy for the volatile oil samples.

Both the extended and the lumped models have an AARE of nearly 4% followed by Bandyopadhyay and Sharma's model (2011) and Elsharkawy's (2003) model; the SRK-EOS has nearly twice the AARE of the newly proposed model. AlQuraishi's (2009) model has an AARE of 12% because the model is based on methane and neglects the effect of heavy and intermediate components, whose contribution is highly significant in the reservoir and production performance of volatile crudes. Jarrahian et al. (2015) model is not suitable for volatile oils; it shows a 34% error in the estimated saturation pressure.

The performance of the extended and lumped models compared to the various methods for the black oil samples (35< C7+<55%) is provided in Figure 6B. The newly proposed models have an AARE close to 10%, followed by Bandyopadhyay and Sharma's (2011) model 14%, the SRK-EOS and PR-EOS 16%, and Elsharkawy (2003) model 17%. AlQuraishi's (2009) model has an AARE of 23%. Jarrahian et al. (2015) model shows a 33% error in estimated saturation pressure even though the authors claim that the model is suitable for black oils.

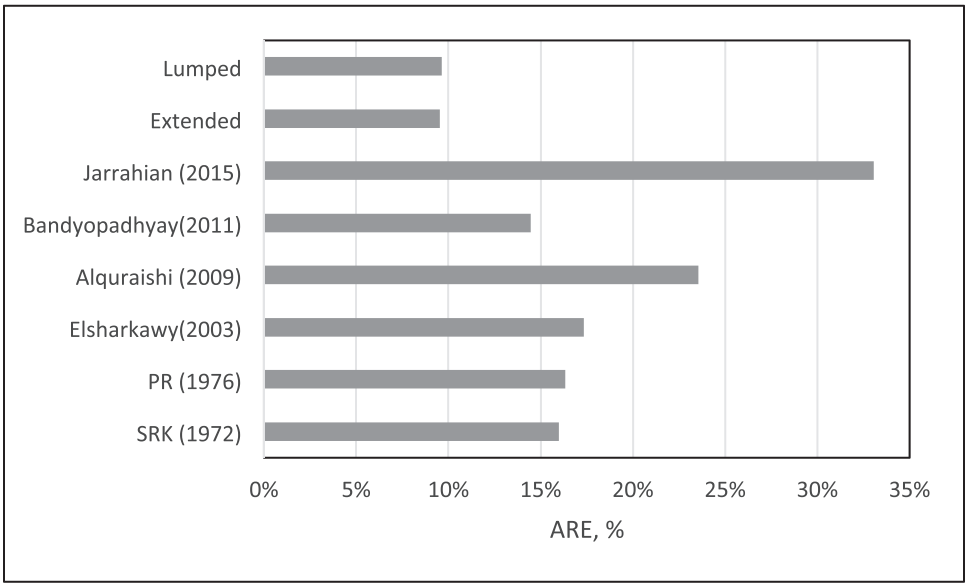

Figure 6B. Comparison of all the models' accuracy for the black oil samples.

Figure 6C shows the error level of all the methods as well as the proposed models for the newly measured crude oil samples at Kuwait University using the PFRC. Again, Jarrahian et al. (2015) model shows a 40% error in estimated saturation pressure.

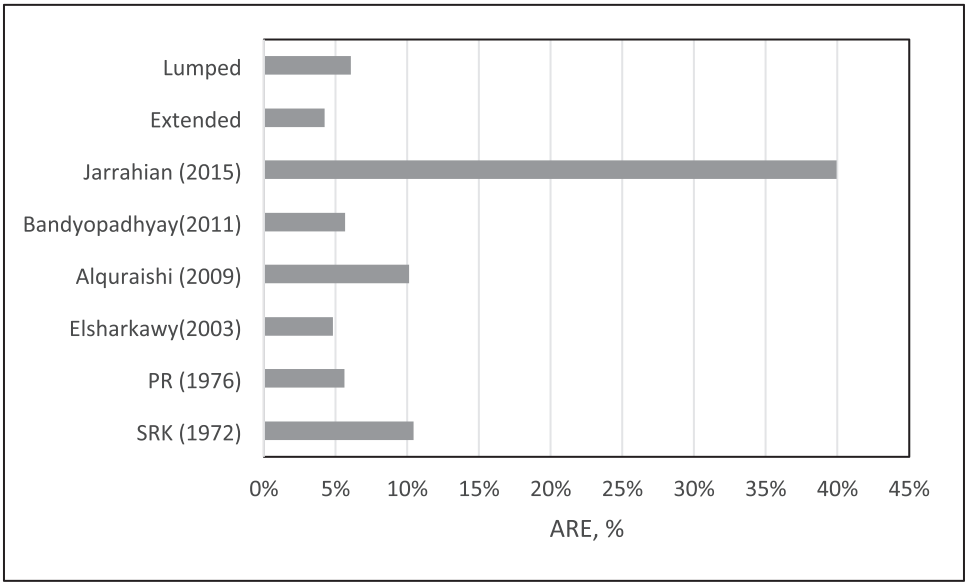

Figure 6C. Comparison of all the models' accuracy for the newly measured samples at KU.

The performance of all published models at low temperature (59oF < T < 71oF) is illustrated in Figure 6D. The low-temperature calculation indicates that Bandyopadhyay and Sharma's4 model has accuracy problems and is not valid at low temperatures because the authors proposed a

temperature-composition related coefficient. Also, Jarrahain et al. (2015) model is not suitable at low temperature. It shows a 32% error in the estimated saturation pressure.

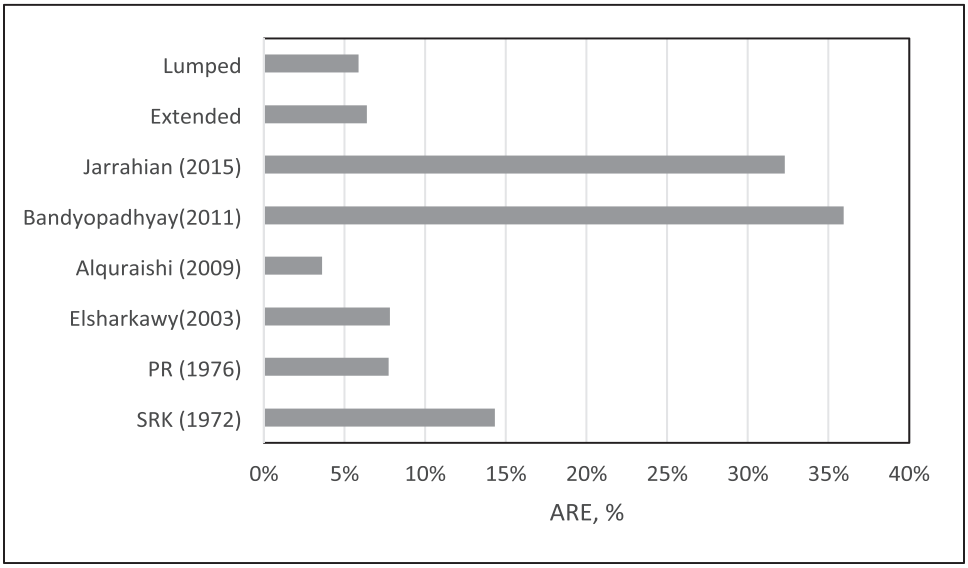

Figure 6D. Comparison of all the models' accuracy for low-temperature oil samples.

The ability of the proposed models to capture the thermodynamic is thoroughly checked against its independent variables. In order to check the validity of the model, the predicted values are compared to the experimental data as well as the predictions by other methods. The model is able to capture the change of the saturation pressure as a function of temperature as illustrated in Figure 7. Two main points are observed; first, the model follows the physical trend predicted by the EOS's. Second, it matches the measured saturation pressures much better than the other methods.

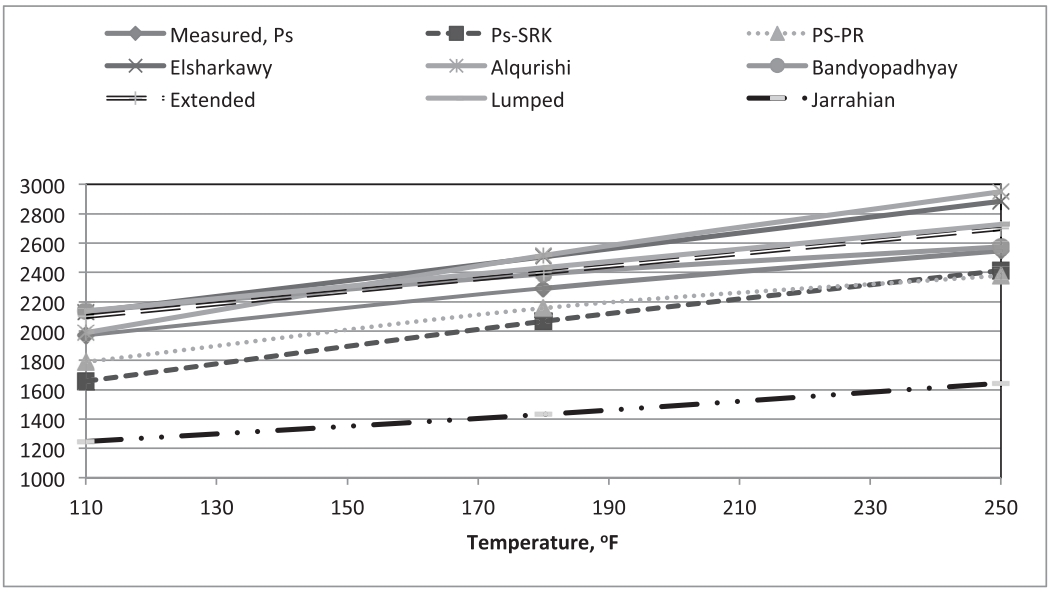

Figure 7. Changes in saturation pressure as a function of temperature for the different models (Sample #70).

Conclusion

In this paper, two models are offered to estimate the saturation pressure of a variety of crude oils when measurements are unreliable or samples are unavailable. The two models are developed using compositional data and saturation pressure measurements from a large data bank of a 231 crude oil samples comprising literature data, and newly measured and reported data. The input parameters in the first model are the extended hydrocarbon and non-hydrocarbon molar percentages and reservoir temperatures. The lumped model uses hydrocarbon fractions of intermediate, and heptane plus fractions in addition to its properties, and the reservoir temperature as input parameters. The accuracy of the two models has been tested and compared to published correlations as well as the SRK-EOS and the PR-EOS, in which all models use compositional data as the input parameters. The comparison indicates that the two models are much more accurate than all the published methods. The validity of both models has also been tested using various types of crude oils samples and compared to experimentally measured saturation pressures and estimates using the EOS as well as the published correlations. The proposed models are physically correct and much simpler than all the published methods. The models do not require tedious computations and eliminate splitting of the plus fraction, characterization of the pseudo-components that are required for the EOS calculations.

Acknowledgment

The authors thank the General Facility Lab at Kuwait University for their cooperation and conducting the compositional and saturation pressure measurements of the 7 new samples described in this paper using Petroleum Fluid Research Center (PFRC) project no. GE 0107/.

Nomenclature

Ps	Saturation pressure
BPP	Bubble-point pressure
EOS	Equation of state
AARE	Average absolute relative error
AAR	Average absolute error
X_i	The mole fraction
SEE	Standard Error of Estimation
R2	Correlation Coefficient
Mw	Average molecular weight
γ_{C7+}	Heptanes plus-fraction
?	The method produces unreasonable results as indicated in the appendix.

References

Ahmadi, M. A., Zendehboudi, S, James, L., Elkamel, A., Dusseault, M., Chatsiz, I. & Lohi, A., 2014, New Tools to determine Bubble Point Pressure of Crude Oils: Experimental and Modeling Study, Journal of Petroleum Science and Engineering, v.123, 204-216.

Ahmed, T., 2011, Splitting and lumping schemes of the plus fraction, working guide to vapour-liquid phase equilibria calculations, Chapter 9, Hydrocarbon Phase Behaviour, Gulf Publishing Co. 111-126.

Al-Marhoun, M.A. 1985. Pressure-Volume-Temperature Correlations for Saudi Crude Oils. Presented at the SPE Middle East Oil Technical Conference and Exhibition, Bahrain, 11–14 March. SPE-13718.

AlQuraishi, A. A., 2009, Determination of crude oil saturation pressure using linear genetic programing, Energy & Fuel, 23, 884-887.

Bandyopadhyay, P. & Sharma, A., 2011, Development of a new semi analytical model for prediction of bubble point pressure of crude oils, Journal of Petroleum Science and Engineering, Volume 78, Issues 3–4, September 2011, Pages 719-731.

Becker, P. J., Celse, B., Guillaume, D., Dulot, H. & Costa, V., 2015, Hydrotreatment modelling for variety of VGD feed stocks: a continuous lumping approach, Fuel, 139, 133-143.

behaviour of aC1/nC24 binary mixture. SPE Reserv. Eng., 271–281.

Bjorlykke, O.P. & Firoozabadi, A., 1992, Measurement and computation of near-critical phase

Coats, K.H. & Smart, G.T., 1986, Application of regression base EOS PVT Program to laboratory data, SPERE, May 277-299.

comprising North Sea reservoir fluids and injection gases. J. Pet. Technol. Nov., 1221–1233.

Elsharkawy, A. M., 2003, An empirical model for estimating the saturation pressures of crude oils, Journal of Petroleum Science and Engineering 38 (2003) 55-77.

Elsharkawy, A.M., 2002, Predicting the dew point pressure for gas condensate reservoirs:

Emera, M. & Samara, H., 2005, Use of genetic algorithm to estimate CO2-oil minimum miscibility pressure-a key parameter in design of CO2 miscible flood, J. Pet. Sci. Eng., Vol. 46, issue 1-2, 37-52.

empirical modelsand equations of state. Fluid phase Equilibria. 193 (1– 2), 147–166.

equation ofstate in engineering and research, in: K.C. Choa, R.L. Robinson Jr. (Eds.),

Farasat, A., Shokrollahi, A., Arabloo, M., Gharagheizi, F. & Mohammadi, A., 2013, toward an intelligent approach for determination of saturation pressure of crude oil, Fuel Processing Technology 115 (2013) 201-214.

Gharbi, R.B.C. & Elsharkawy, A.M., 1999, Neural Network Model for Estimating the PVT Properties of Meddle East Crude oils, SPE Reservoir Eval. Eng. 2 (3), 255-265.

Gholami, A., Asoodeh, M. & Bagheripour, P., 2014, How committee machine with SVR and ACE estimates bubble point pressure of crudes, Fluid Phase Equilibria, Volume 382, 25 November 2014, Pages 139-149.

Gulf Publishing,Houston

Heidaryan, E. & Moghadasi, J., 2011, Crude saturation pressure through imperial correlation, Thermodynamics 2011, Athens, 31 August- 3 September 2011.

Jarrahian, A., Moghadsi, J. & Heidaryan, E., 2015, Empirical estimating of black oil bubblepoint (saturation) pressure, J. Petroleum Science and engineering, (126), 69-77.

Katz, D.L. & Firoozabadi, A., 1978, Predicting phase behaviour of condensate/crude-oil system

Peng, D. y. & Robinson. D. B., 1976, A new two-constant equation of state, Ind. Eng. Chem. Fund. 15, 59-63.

producingvolatile oil, AIME 213, 59-65.

Rosengger, L., Wu., R.1990, Integrated PVT data characterization- lessons from four case histories, J. Can. Per. Tech., 38, (13), (paper 97-05)

Soave, G. 1972, Equilibrium constants from a modified Redlich-Kwong equation of state, Chem. Eng. Sci. 27, 1197-1203.

Tale, M., Alquraishi, A. & Al Mushaigeh, E. 2009, New model for crude oil saturation pressure prediction using alternation conditional expectation, Offshore Mediterranean Conf. & Exhibit. Italy 25-27, 2009.

Vogel, J.R. & Yarborough, L. 1980, the effect of nitrogen on phase behavior and phase properties of reservoir fluids, SPE 8815.

Whitson, C. H., 1980, Characterizing hydrocarbon plus fraction, SPEJ, 24 (4), 683694-.

with different types of mixing rules. Fluid phase Equilibria. 91, 1– 29.

Appendix A

Equation of State Calculation

Many cubic equation of state are widely used for saturation pressure calculations. None of the available EOSs can be singled out as the most superior to predict the saturation pressure61. The accuracy of the EOS's calculations depends on the following:

1. The type of EOS used, PR, SRK, etc.
2. The splitting scheme used to divide the heavy hydrocarbon fraction into sub-fractions.
3. The correlation used to estimate the critical properties of the sub-fraction.
4. The inclusion of the binary interaction number ($K_{i,j}$).

In this study, two equations of state calculation of saturation pressure are considered, Soave-Redlich-Kwong (SRK-EOS) and Peng-Robinson (PR-EOS).

SRK-EOS has the following from:

$$P = \left(\frac{RT}{V-b}\right) - \left(\frac{\alpha\alpha}{V(V+b)}\right)$$

where P is the pressure, V the molar volume, T the absolute temperature, and R the universal gas constant. The parameter a is a dimensionless factor, which becomes unity at critical pressure. At the bubble point pressure, the composition of the liquid phase (Xi) equals the overall composition (Z_i) of the reservoir fluids. This leads to the following expression:

$$\sum Zi * Ki = 1$$

where ki is the equilibrium ratio for the component calculated from the equation of state. Thus, the saturation pressure (Pb) is calculated from the above equations using the following expression:

$$P_d = \sum \frac{f_i^l}{\varphi_i^v}$$

where is the vapor fugacity coefficient and is the liquid fugacity of the ith component, which is calculated from the equation of state.

PR-EOS has the following form:

$$P = \left(\frac{RT}{V-b}\right) - \left(\frac{\alpha\alpha}{V(V+b)+b(V-b)}\right)$$

The difference between SRK-EOS and PR-EOS lies in calculation of the parameters, a, b, and a. This difference results in that the fugacity, fugacity coefficient, and compressibility factor calculated from each of the equations of state are quite different. Therefore, the results from calculating DPP using SRK-EOS and PR-EOS are not the same.

Splitting the plus fraction

Hydrocarbon plus fraction that comprises a significant portion of the reservoir fluids creates problems when predicting thermodynamic and phase behavior of these fluids using equation of states. These problems arise from the difficulty of properly characterizing the plus fraction. Several splitting schemes are proposed to divide the hydrocarbon plus fraction into sub-fraction, (Pedersen et al., 1989), (Katz, Firoozabadi, 1978), and (Yarborough, 1978). The logarithmic distribution proposed by Pedersen et al. (1989) is considered in this study.

Characterizing the sub-fraction

Equations of state calculations require critical pressure (P_c), critical temperature (T_c), and eccentric factor (w) for every component forming the hydrocarbon fluid. Critical properties and eccentric factor are well-documented for pure components. However, critical properties for the sub-fraction are estimated from correlations. In this study (Pedersen et al., 1989), correlation is used to calculate the critical properties of the sub-fraction.

Binary interaction

To use the SRK or PR equations of state to predict saturation pressure of complex hydrocarbon mixture, it is necessary to correct for the binary interaction ($K_{i,j}$) between different components by means of empirically derived interaction numbers. The use of binary interaction in equations of state calculations is controversial. Some researchers neglected it for hydrocarbon components, used standard values for EOS (Whitson and Brule, 2000), and others used binary interaction, which are function of temperature (Varotsis et. al., 1986), pressure (Voros and Tassios, 1985), or compositions (Bjorlykke and Firoozabadi, 1992). In this study, the objective is not to find the optimum binary interaction that leads to accurate prediction of the saturation pressure. Therefore, the interaction number is set to zero.

Appendix B

Statistical Analysis

To study of the proposed models against the other methods, the following statistical parameters have been calculated. The average percent relative error (ARE):

$$ARE\% = \frac{100}{N_d}\sum_{i=1}^{N_d}\left(\frac{p_i^{exp} - p_i^{calc}}{p_i^{exp}}\right)$$

ARE% is a measure of bias; a value of zero indicates an unbiased distribution of the error.

The arithmetic average of the absolute values of the relative errors (AARE):

$$AARE\% = \frac{100}{N_d}\sum_{i=1}^{N_d}\left(\frac{p_i^{exp} - p_i^{calc}}{p_i^{exp}}\right)$$

The correlation determination R^2 a measure of the precision of the fit of the data:

$$R^2 = 1 - \frac{\sum_{i=1}^{N_d}\left(P_i^{exp} - p_i^{calc}\right)^2}{\sum_{i=1}^{N_d}\left(p_i^{exp} - p_{mean}^{exp}\right)^2}$$

The standard error of estimates (SEE) is the square root of the mean square error, which is the variance of the true residuals. It is expressed as

$$SEE = \left[\frac{\left\{\sum_{i=1}^{N_d}\left(\frac{\left(P_i^{exp} - p_i^{calc}\right)}{P_i^{exp}}\right)^2\right\}}{(N_d - v - 1)}\right]^{0.5}$$

where v is the number of variables.

Appendix C

In this appendix, sample calculations are presented to show the deficiency of some of the published methods.

Input parameters:

N_2	CO_2	H_2S	C_1	C_2	C_3	C_4	C_5	C_6	C_{7+}	GR.C7+	MWC7+	T, °F	Ps, psia
0.65	0.02	0	45.02	12.45	8.93	6.03	3.02	1.44	22.44	0.81	184	140	3002

(Ahmadi et al., 2014)

Ahmadi et al. proposed an 8-step calculation (copied from their paper) to estimate the BPP as follows:

$$BPP = A \times Mw_{C7+} - \frac{B}{C_{7+}} + C \times \text{Vol./Inter.} + D \times SG_{C7+} + \frac{E}{SG_{C7+}} + \frac{F}{Mw_{C7+}} + T \times 505.967 + \frac{2.45789 \times 10^6}{T} + \frac{G}{\text{Vol./Inter.}} \quad (5)$$

$$A = 1488.46 - SG_{C7+} \times 1087.64 - \frac{601.512}{SG_{C7+}} + 1670.58 + T \times 0.40771 + \frac{6345.73}{T} + \frac{8.72863}{\text{Vol./Inter.}} \quad (6)$$

$$B = \frac{4132.53}{\text{Vol./Inter.}} + \frac{6.1977 \times 10^7}{Mw_{C7+}} + T \times 3181.39 + \frac{1.06393 \times 10^8}{T} \quad (7)$$

$$C = \frac{20964.7}{C_{7+}} - \frac{1.76162 \times 10^6}{Mw_{C7+}} - T \times 19.1963 - Mw_{C7+} \times 21.5427 + \frac{12851.5}{SG_{C7+}} - \frac{712613}{T} - 3477.49 + SG_{C7+} \times 9532.73 \quad (8)$$

$$D = 1.05345 \times 10^{+06} - \frac{1.50748 \times 10^8}{Mw_{C7+}} - T \times 676.048 - \frac{1.20252 \times 10^7}{T} - \frac{12178.2}{\text{Vol./Inter.}} \quad (9)$$

$$E = 641357 - \frac{1.02891 \times 10^8}{Mw_{C7+}} - T \times 301.034 - \frac{1.91446 \times 10^6}{T} - \frac{3873.62}{\text{Vol./Inter.}} \quad (10)$$

$$F = 2.51471 \times 10^{+08} + T \times 25332.5 + \frac{3.47893 \times 10^8}{T} - \frac{244573}{\text{Vol./Inter.}} \quad (11)$$

$$G = 20125.6 - T \times 23.9271 - \frac{703193}{T} \quad (12)$$

Ahmadi et al. define the Vol. /Inter. as the mole percentage ratio of the volatile (C_1& N_2) to the intermediate components (C_2 to C_6, CO_2 and H_2S). Application of the above equations (6 through 12 and 5, respectively) uses the input parameters results in the following.

Vol./Inter.	A	B	C	D	E	F	G	BPP
1.43211	1643.9	1545062	-271.127	45122.71	23642.47	2.57E+08	11753	1,794,123

The calculated saturation pressure (BBP) from Eq.5 is 1,794,123 psia, which is unreasonable. This indicates a deficiency in the model.

(Gholami et al., 2014)

Gholami et al. presented a three-step calculation to estimate the BPP. They proposed an alternating conditional expectation (ACE) to correlate the bubble pint pressure to input variables through approximating the optimal transformation of the input variables using their equation 15.

$$T_r(M) = \sum_{i=0}^{5} B_i M^i \quad (15)$$

where M is non-transformed input of model coefficients of Bo through B5 for each input given in Table 1 in their paper.

Table 1: Polynomial coefficients for determining optimal transformation of each input variables

M	B_0	B_1	B_2	B_3	B_4	B_5
N_2	0.0185030779	-0.2916633775	1.3819288142	-2.3399985776	1.5543841420	-0.3601815110
CO_2	0.0617156522	-0.0398373616	-0.0038619272	0	0	0
H_2S	0.0506358597	-0.1258546745	-0.0132294174	0	0	0
C_1	1.3087460313	-0.0396562495	0	0	0	0
C_2	0.2231049163	0.0075432380	-0.0047256448	0	0	0
C_3	1.0696557789	-0.1702671404	0	0	0	0
C_4	0.1072162412	-0.0427491659	0.0060729584	-0.0004117921	0	0
C_5	0.5069895059	-0.1501134188	0.0062648526	-0.0015254204	0	0
C_6	0.3348331271	0.3124433847	-0.4085365491	0.1395671394	-0.0202419290	0.00106663389
C_{7+}	4.0459303201	-0.0994388167	0	0	0	0
SG_{7+}	239.7204527985	-1175.42286924	2135.5051639487	-1709.8467582	509.0285892159	0
MW_{C7+}	0.3722804910	-0.0134792734	0.0012182843	-0.0000004112	0.0000000004	0
T	-2.7706165514	0.0346240882	-0.0001373443	0.0000001836	0	0

Application of Equation 15 and the compositional data of the previous example resulted in the following coefficients for the input values.

N_2	0.00584
CO_2	0.060917
H_2S	0.050636
C_1	-0.47658
C_2	-0.41547
C_3	-0.45083
C_4	-0.02003
C_5	0.068769
C_6	0.273921
C_{7+}	1.814523
SG.C7+	-0.0197
MWC7+	37.03525
T., F	-0.11139

The sum of optimal transformations of input parameters is achieved from equation (16).

$$Tr(P_b) = Tr(N_2) + Tr(CO_2) + Tr(H_2S) + Tr(C_1) + Tr(C_2) + Tr(C_3) + Tr(C_4) + Tr(C_5) + Tr(C_6) + Tr(C_{7+}) + Tr(SG_{C7+}) + Tr(MW_{C7+}) + Tr(T) \quad (16)$$

Application of Equation (16) using the coefficient in the above table resulted in Tr(Pb) = 37.8159.

The bubble pint pressure is calculated from curve fitting, optimal formulation between sum of transformations, and Pb, using equation (17).

$$P_b = (57.0840387741\, x(Tr(P_b))^2) + (1166.9102304199\, x(Tr(P_b))) + 2207.3573204358 \quad (17)$$

Application of Equation (17) resulted in saturation pressure (Pb) = 127,967 psia, which is unreasonable, compared to the measured one is 3002 psia. This indicates that there is a deficiency in the model.

(Jarrahian et al., 2015)

Jarrahian et al. proposed the Equation (18) to estimate the saturation pressure:

$$P_{sat} = A_0 exp\big(A_1 Z_{N_2} + A_2 Z_{co_2} + A_3 Z_{H_2S} + A_4 Z_{C_1}^{A_5} + A_6 \textstyle\sum_2^6 Z_{C_1} + A_7 Z_{C_{7+}}^{A_8} \gamma_{C_{7+}}^{A_9} MW_{C_{7+}}^{A_{10}} + A_{11}\,(T - 459.67)\big) \quad (18)$$

where the coefficients A0 through A11 are given in Table 2 in their paper.

Table 2. coefficient of Eq. (18).

Coefficient	Tuned Coefficient
A_0	$8.76381902810839 \times 10^{-01}$
A_1	$1.03542031515935 \times 10^{-01}$
A_2	$2.85220583982046 \times 10^{-02}$
A_3	$9.57159522979151 \times 10^{-03}$
A_4	$2.05038939147643 \times 10^{+00}$
A_5	$2.50151158241171 \times 10^{-01}$
A_6	$-1.83210325410041 \times 10^{-03}$
A_7	$2.63492761796153 \times 10^{+00}$
A_8	$-5.44923287210873 \times 10^{-02}$
A_9	$4.23424455043480 \times 10^{-01}$
A_{10}	$-5.44298830074401 \times 10^{-05}$
A_{11}	$1.97788001541373 \times 10^{-03}$

Application of Equation (18) resulted in saturation pressure (Ps) = 1812 psia, compared to the measured one of 3002 psia. This indicates that model has inaccuracy problem. This inaccuracy has been the pattern in all the crude oil samples shown in Table 2 and figures 6A through 6D.

Submitted: 06/12/2016
Revised : 15/03/2017
Accepted : 19/03/2017